Supplemental Figure 1 Muro et al

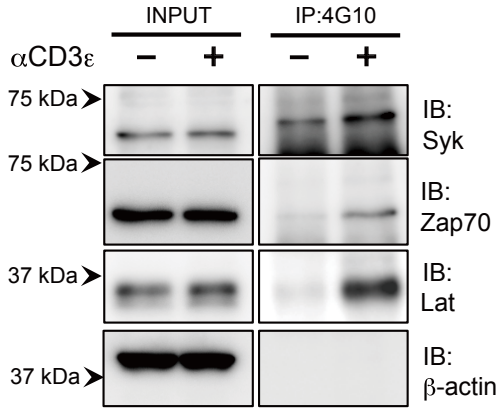

Supplemental Figure 1. TCR-induced tyrosine phosphorylation of Syk as well as Zap70 in γδT cells

γδT cells isolated from neonatal WT mice were stimulated with anti-CD3ε antibody (2C11) for 2 min. Cell lysates were immunoprecipitated with antiphosphotyrosine antibody (4G10) followed by immunoblotting with the indicated antibodies. Representative immunoblotting from two independent experiments was shown.

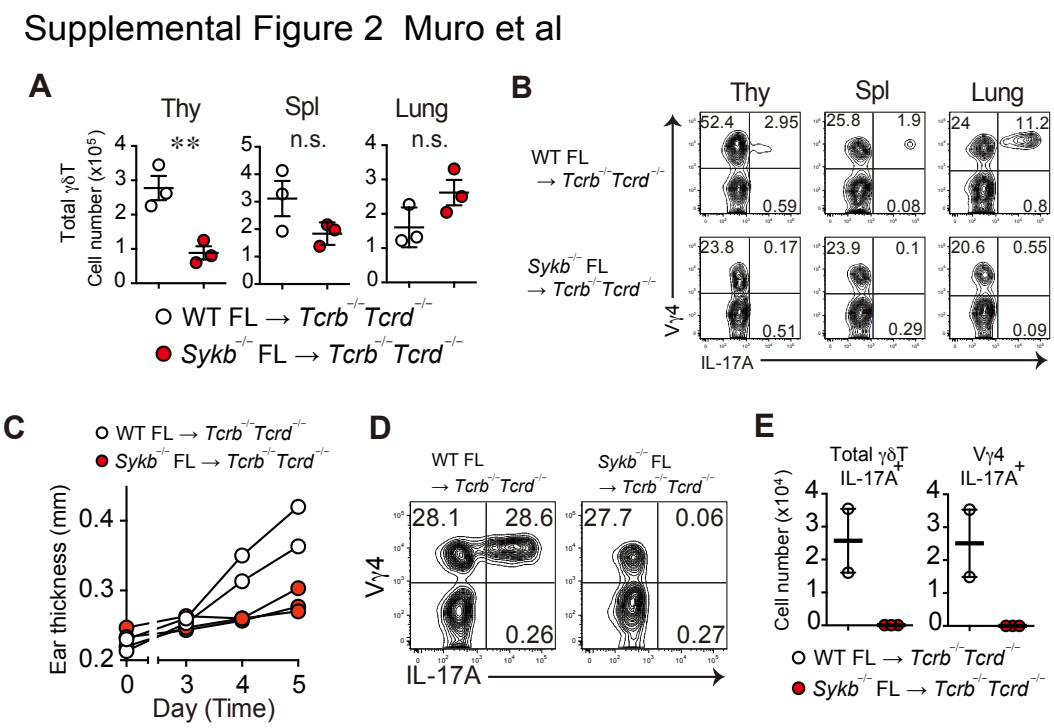

Supplemental Figure 2. IL-17 production of Syk-deficient γδT cell in the periphery of adult mice

(**A**) Absolute numbers (per mouse) of total γδT cells in thymus (Thy), spleen (Spl), and lung from indicated fetal liver (FL) chimeric mice are shown (lower, n = 3). The mice were analyzed 8 weeks after FL cell transplantation. (**B**) Representative flow cytometry profiles for cell surface Vγ4 and intracellular IL-17A expression in γδT cells from the indicated tissues after stimulation with PMA and ionomycin. Symbols and lines in graphs indicate individual mice and mean, respectively. Error bars indicate SEM. $*p < 0.05$; $**p < 0.01$; n.s., not significant, by unpaired t-test. (**C**-**E**) FL chimeric mice were treated daily for 5 days with IMQ cream on the ear (WT FL n = 2, *Sykb*$^{-/-}$ FL n = 3). Kinetics of IMQ-induced ear swelling (**C**), flow cytometry analysis of IL-17^{+} cells in γδT cells from ear-draining lymph nodes at day 5 (**D**), and the number of IL-17^{+} γδT cells from ear-draining lymph nodes at day 5 (**E**). Data represent single experiment.

Supplemental Figure 3 Muro et al

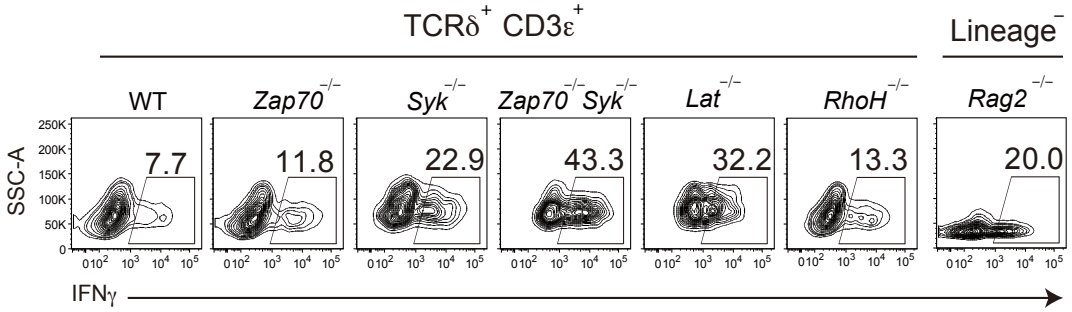

Supplemental Figure 3. IFNγ-producing potential of immature γδT cells and DN thymocytes

Thymocytes from indicated mice were stimulated with PMA plus ionomycin for 4 h. Contour plots show intracellular staining for IFNγ production in γδT cells from *Zap70*$^{-/-}$, *Sykb*$^{-/-}$, *Zap70*$^{-/-}$ *Sykb*$^{-/-}$, *Lat*$^{-/-}$ or *Rhoh*$^{-/-}$ mice (n = 4-26), or CD11b^{-} CD11c^{-} CD49b^{-} TER119^{-} B220^{-} Gr-1^{-} (lineage-negative) cells from *Rag2*$^{-/-}$ mice (n = 4). Data represent the combined result of six independent experiments.

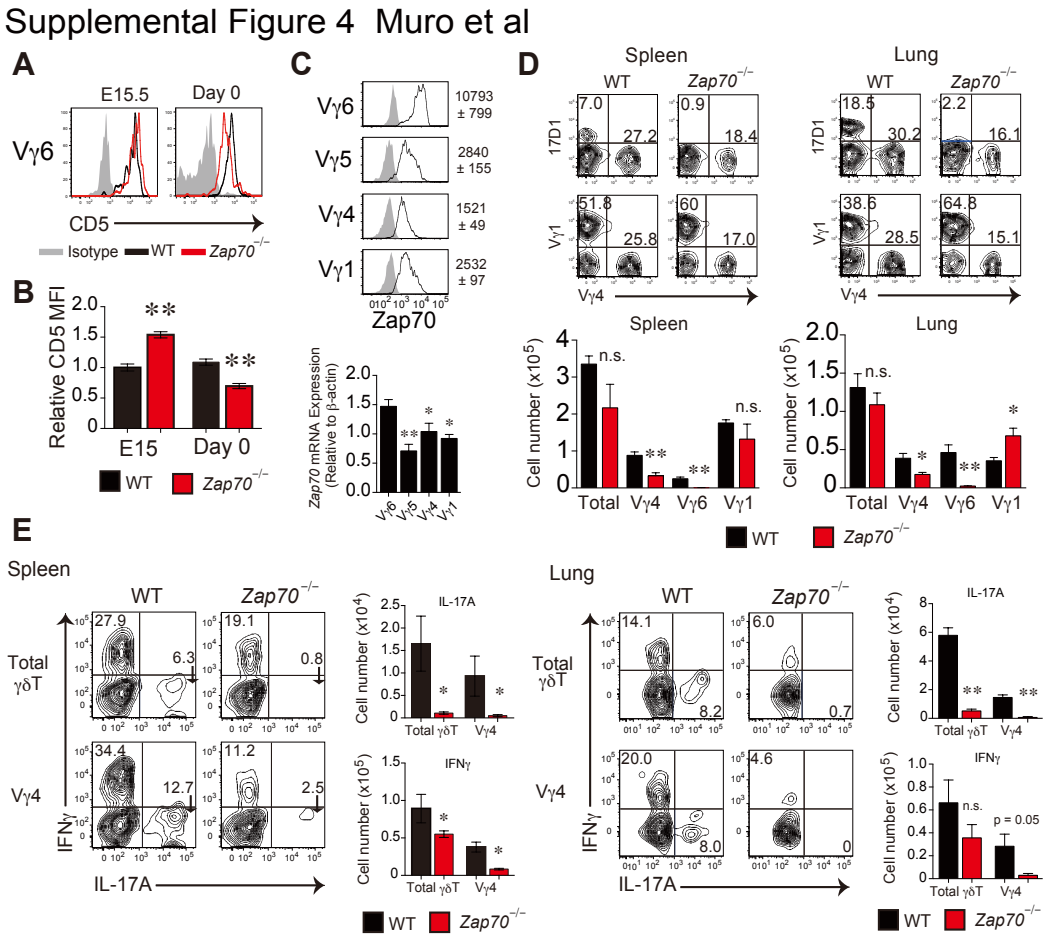

Supplemental Figure 4. Requirement of Zap70 in γδT cell development

(**A** and **B**) Flow cytometry analysis of CD5 expression in thymic Vγ6$^+$ γδT cells from WT or *Zap70*$^{-/-}$ mice at E15.5 (n = 5–10) or day 0 (n = 3). Relative MFI of CD5 expression is shown. (**C**) Zap70 protein (top) and mRNA (bottom) expression in thymic γδT cell subsets from neonatal WT mice. The numbers beside the flow cytometry histograms indicate MFI (mean ± SE) of Zap70 protein expression (n = 4). Zap70 mRNA expression levels were normalized to β-actin mRNA (n = 3). (**D**) Representative flow cytometry profiles for Vγ chains in γδT cells from indicated tissues (upper). Absolute numbers (per mouse) of indicated γδT cell subsets and total γδT cells are shown (lower, n = 4–6). (**E**) Intracellular staining for IL-17A and IFNγ production in indicated spleen or lung γδT cells from 5-week-old WT or *Zap70*$^{-/-}$ mice (n = 3–4). Graphs show the absolute number of IL-17A$^+$ or IFNγ$^+$ γδT cells. All graphs indicate the mean ± SEM. ∗p < 0.05; ∗∗p < 0.01; n.s., not significant, by unpaired t-test. Data represent more than two independent experiments (**D** and **E**) or single experiment (**A-C**).

Supplemental Figure 5 Muro et al

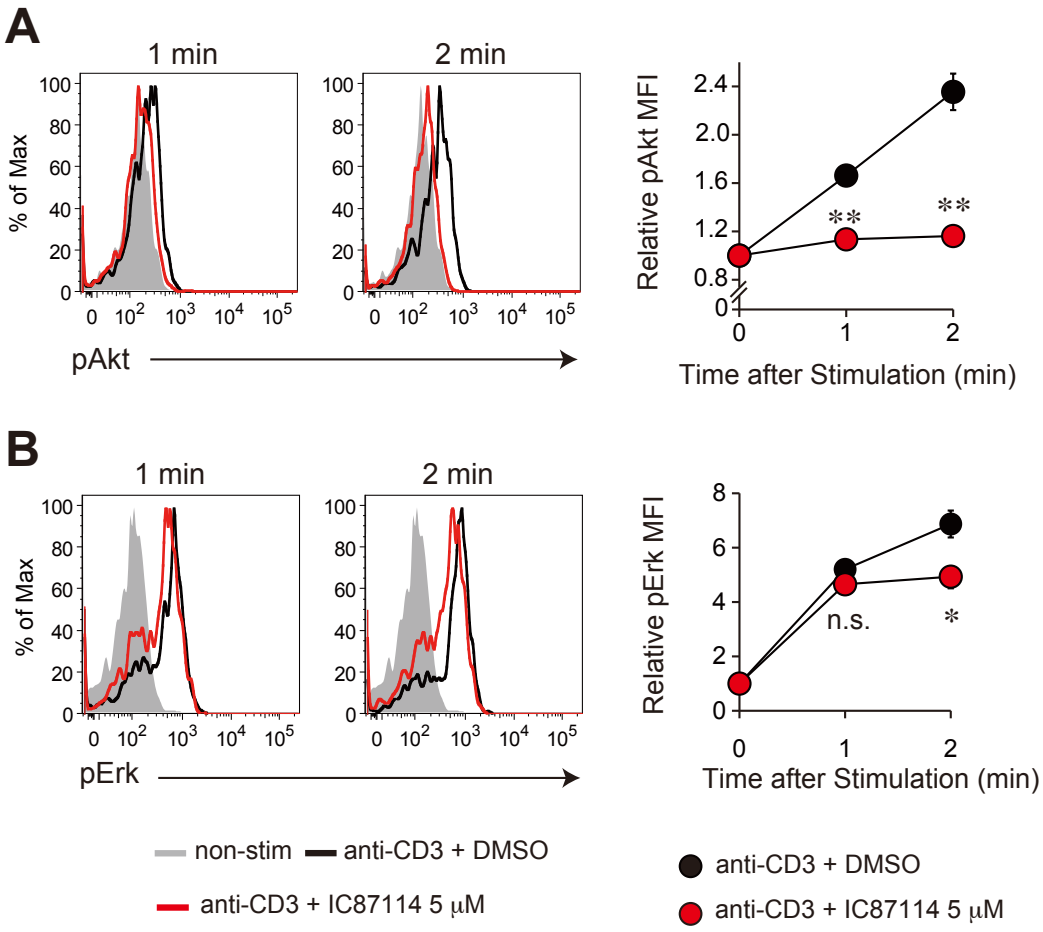

Supplemental Figure 5. TCR-induced Akt phosphorylation in γδT cells is dependent on PI3K activity

(**A** and **B**) Representative flow cytometry profiles of TCR-induced phosphorylation of Erk (**A**) or Akt (**B**). Cells were pretreated with IC87114 at a final concentration of 5 μM for 1 h. Graphs show relative MFI of phospho-Erk or phospho-Akt (n = 3). All graphs indicate the mean ± SEM. ∗p < 0.05; ∗∗p < 0.01; n.s., not significant, by 2-way ANOVA. Data represent single experiment.

Supplemental Figure 6 Muro et al

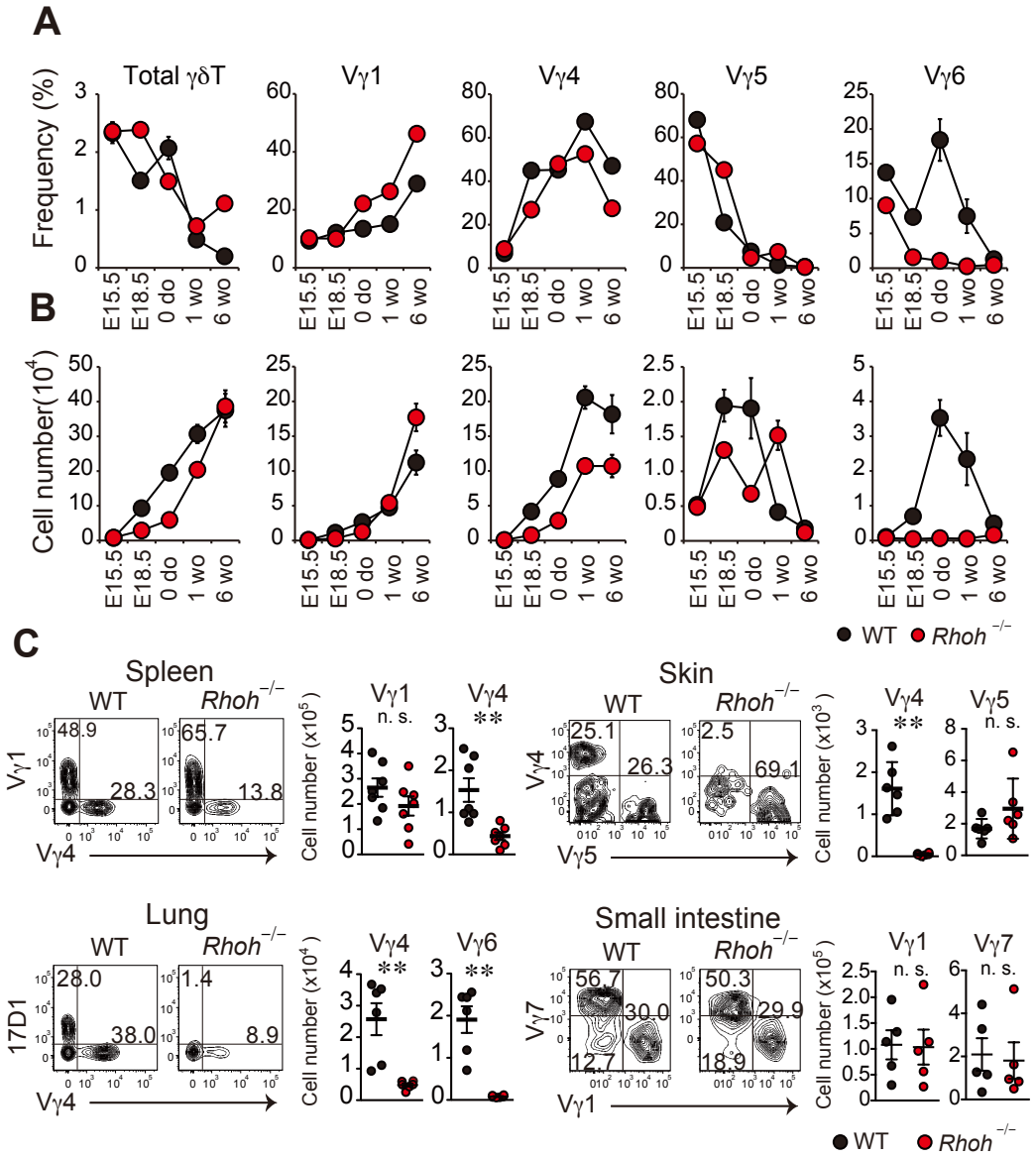

Supplemental Figure 6. γδT cell development in RhoH-deficient mice

(**A**) Frequency of total γδT cells (% of total thymocytes) and indicated γδT cell subset (% of total γδT cells) from indicated age of WT or *Rhoh*$^{-/-}$ mice (n = 5–9). (**B**) Absolute number of indicated γδT cells (per mouse), as described in A. Graphs indicate mean ± SE. (**C**) Representative flow cytometry profiles for Vγ expression in γδT cells from indicated tissues of 6-week-old WT or *Rhoh*$^{-/-}$ mice. Graphs indicate the cell number (per mouse) of indicated γδT cell subsets in individual mice (circles) and their mean ± SE (n = 5–7). All graphs indicate the mean ± SEM. ∗p < 0.05; ∗∗p < 0.01; n.s., not significant, by unpaired t-test. Data represent two independent experiments (**C**) or the combined result of five independent experiments (**A** and **B**).

Supplemental Figure 7 Muro et al

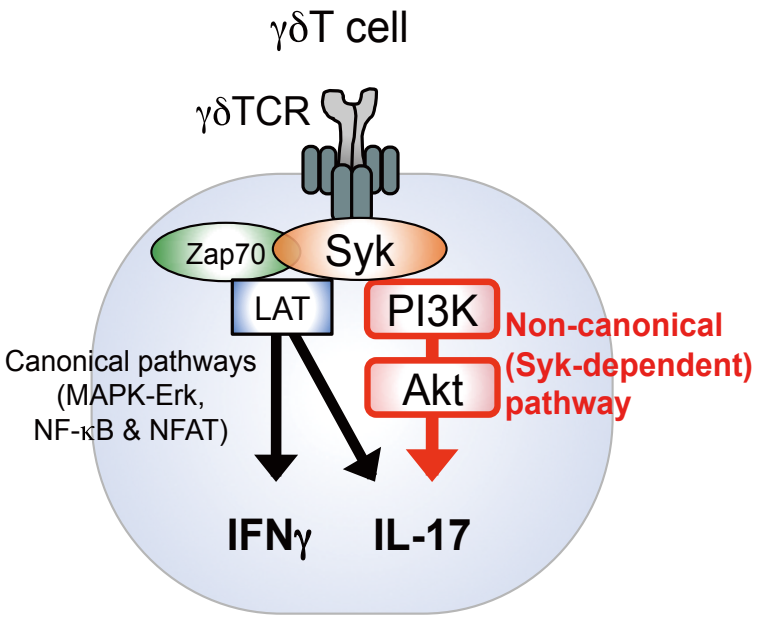

Supplemental Figure 7. A schematic model of γδT17 cell differentiation regulated by Syk-dependent TCR signals

In response to γδTCR stimulation, Syk activates LAT-dependent canonical pathway, including the MAPK cascade, and Lat-independent non-canonical pathway mediated by the PI3K-Akt axis. The former acts as a mainstream signal, which is required for γδT cell maturation and differentiation toward IFNγ-producing cells, while the latter induces alternative differentiation program toward γδT17 through the expression of transcription factors Sox13 and RORγt.

Supplemental Table 1. Summary of mouse γδT cell subsets

Vγ chain		Tissue distribution	Cytokine production
Heilig and Tonegawa's nomenclature	Garman's nomenclature		
Vγ1	Vγ1.1	lymphoid tissue, liver	IFNγ
Vγ4	Vγ2	lymphoid tissue, liver, lung, dermis	IFNγ or IL-17
Vγ5	Vγ3	dermis	IFNγ
Vγ6	Vγ4	lung, uterus, tongue	IL-17
Vγ7	Vγ5	intestine	IFNγ